


ORIGINAL ARTICLE

Open Access



Isolation, identification and phylogenetic analysis of a lumpy skin disease virus strain from diseased beef cattle in China

Xinwei Yuan^{1,2†}, Xiaowen Xu^{1,2†}, Qingni Li^{1,2†}, Chen Wang^{1,2}, Zhijie Xiang^{1,2}, Yingyu Chen^{1,2,3}, Changmin Hu^{1,2,3*} and Aizhen Guo^{1,2,3*} 

Abstract

Lumpy skin disease (LSD) is a highly contagious viral disease in cattle caused by lumpy skin disease virus (LSDV), which belongs to the genus *Capripoxvirus* (CaPVs) within the family *Poxviridae*. Since its first outbreak in China in August 2019, LSD has spread widely across mainland China, posing significant threats to the cattle industry. This study aimed to isolate and identify a clinical strain of LSDV *via* Vero cells. Skin tissue samples from lump lesions were homogenized and inoculated onto cell cultures. After 7 passages, the inoculated cells exhibited typical cytopathic effects (CPEs). PCR amplification of the *LSDV132* gene confirmed the presence of LSDV nucleic acid. In addition, quantitative PCR (qPCR) demonstrated a significant increase in viral copy number over time. Transmission electron microscopy (TEM) revealed typical brick-shaped viral particles. Furthermore, an indirect immunofluorescence assay (IFA) of infected Vero cells exhibiting CPEs produced a positive reaction with antiserum from cattle naturally infected with LSDV. Additionally, nucleotide similarity analysis of 123 LSDV strains revealed a high degree of similarity (98.4%–100%) among different geographic lineages. Nucleotide sequencing and recombination analysis of the *LSDV011* gene from LSDV/China/HB01/2020 revealed close similarity to Asian strains and revealed a recombination event. Furthermore, similarity plot analysis confirmed two genomic exchange sites at nucleotide positions 120 and 762 within the *LSDV011* gene. Recombination events between 65 Asian LSDV strains and 13 goatpox virus (GTPV) strains have raised safety concerns regarding the use of attenuated goatpox vaccines, highlighting the need for novel and safer LSDV vaccines. In summary, this study successfully isolated a clinical LSDV strain, demonstrating its evolutionary status and providing crucial insights for LSD control in the cattle industry.

Keywords Lumpy skin disease (LSD), Lumpy skin disease virus (LSDV), Recombination, Virus isolation, Phylogenetic analysis

Handling editor: Yifei Lang.

[†]Xinwei Yuan, Xiaowen Xu and Qingni Li contributed equally to this work.

*Correspondence:

Changmin Hu

hcm@mail.hzau.edu.cn

Aizhen Guo

aizhen@mail.hzau.edu.cn

Full list of author information is available at the end of the article



© The Author(s) 2025. **Open Access** This article is licensed under a Creative Commons Attribution 4.0 International License, which permits use, sharing, adaptation, distribution and reproduction in any medium or format, as long as you give appropriate credit to the original author(s) and the source, provide a link to the Creative Commons licence, and indicate if changes were made. The images or other third party material in this article are included in the article's Creative Commons licence, unless indicated otherwise in a credit line to the material. If material is not included in the article's Creative Commons licence and your intended use is not permitted by statutory regulation or exceeds the permitted use, you will need to obtain permission directly from the copyright holder. To view a copy of this licence, visit <http://creativecommons.org/licenses/by/4.0/>. The Creative Commons Public Domain Dedication waiver (<http://creativecommons.org/publicdomain/zero/1.0/>) applies to the data made available in this article, unless otherwise stated in a credit line to the data.

Introduction

Lumpy skin disease (LSD) is an acute or subacute infectious disease caused by lumpy skin disease virus (LSDV), which poses a serious threat to global cattle health and livestock industry sustainability (Moudgil et al. 2024; Smaraki et al. 2024). The disease is transmitted primarily by blood-sucking insect vectors, including *Stomoxys* spp., mosquitoes (*Aedes aegypti*), and hard ticks (*Rhipicephalus appendiculatus*) (Issimov et al. 2020; Chihota et al. 2003; Shumilova et al. 2022). Direct transmission can occur when ruptured nodules on the skin and mucosal surfaces release high viral loads, with mutual licking among cattle being a major route (Yuan et al. 2023). Bovines are the primary natural hosts of LSDV. The virus can also be transmitted via the placenta, semen, contaminated feed, water, equipment, and veterinary needles (Annandale et al. 2014). Furthermore, long-distance transportation of infected animals or contaminated animal products may facilitate the widespread dissemination of LSDV (Klausner et al. 2017). Ulceration and necrosis of nodules further increase the risk of vector-borne transmission (Lubinga et al. 2013).

Clinically, LSD is characterized by widespread, firm, flat-topped skin nodules measuring 5–50 mm in diameter, which can extend into subcutaneous tissue or even muscle (Abutarbush et al. 2015; Kononov et al. 2019a, b). In its early stages, LSD typically presents with a high fever (up to 41 °C), followed by physiological disorders such as skin nodules, reduced milk yield, stunted growth, abortions, and temporary or permanent infertility in bulls (Di Giuseppe et al. 2024; Hunter et al. 2001).

The World Organization for Animal Health (WOAH) has classified LSD as a notifiable disease (WOAH 2023). LSD originated in southern Africa, specifically in Zambia, where the disease is endemic. A recent study reported ongoing viral circulation and the emergence of novel subgroups, particularly in West Africa and Central Africa (Haga et al. 2024). A systematic review and meta-analysis estimated the pooled prevalence of LSD at 54% (ranging from 6%–89%) between 2007 and 2023, with notably high rates in Zimbabwe (88%) and Egypt (58%) (Abebaw et al. 2024). In addition, a study in the Sidama region of Ethiopia reported high seroprevalence at both herd (81%) and individual (40.8%) levels across three agroecological zones, while farmers demonstrated limited awareness of the disease (Moje et al. 2024). LSD has since spread to Europe and, more recently, across Asia (Data Source: FAO, <https://empres-i.fao.org>). These findings underscore the persistent global burden of LSD and the urgent need for effective surveillance, vaccination, and farmer education.

In August 2019, LSD was first detected in Yili, Xinjiang Uyghur Autonomous Region, China, and subsequently

spread to multiple provinces across the country (Data Source: Veterinary Bulletin of the Ministry of Agriculture and Rural Affairs of China). In China, a fivefold goat dose of the live attenuated goatpox vaccine has commonly been used to immunize cattle herds (Yuan et al. 2024). However, since transboundary trade in cattle has become increasingly common, LSD subsequently spread from China to several countries, including Bangladesh, India, Vietnam, Thailand, Malaysia, and Indonesia, all of which later reported outbreaks (EFSA et al. 2020; Badhy et al. 2021; Sudhakar et al. 2022; Tran et al. 2021; Arjkumpa et al. 2021; Smaraki et al. 2024). To date, the NCBI database has archived the complete genomes of 123 LSDV strains isolated from 22 countries worldwide. A comprehensive phylogenetic and recombination analysis of these viral strains on a global scale is warranted. More importantly, further investigation is needed to determine whether the LSDV/China/HB01/2020 strain isolated in this study, along with other strains from China and neighboring Asian countries, has undergone recombination with the attenuated goatpox vaccine used for cattle immunization.

In this study, a clinical isolate designated LSDV/China/HB01/2020 was obtained from skin tissue samples of diseased beef cattle in Hubei Province, China. To characterize this isolate, we employed PCR, qPCR, IFA, and TEM and conducted phylogenetic analysis on the full-genome sequences of LSDV and GTPV to evaluate potential recombination events. These findings increase our understanding of LSDV genetic diversity in China and provide a foundation for future research on viral evolution, epidemiology, and the development of effective disease control strategies.

Results

Detection and isolation of LSDV from clinical tissue

PCR amplification of the *LSDV132* gene yielded a product of the expected size (379 bp), as visualized by 1% agarose gel electrophoresis (Supplementary Fig. 1A). The PCR product was subsequently subjected to Sanger sequencing, and sequence analysis confirmed 100% identity with the *LSDV132* gene, with no mutations or deletions detected (Supplementary Fig. 1B). These results confirmed the presence of LSDV in the clinical samples.

Homogenized skin tissue suspensions were inoculated onto Vero cell monolayers, and cytopathic effects (CPEs) were observed daily under an inverted microscope. Significant CPEs for both GTPVs and LSDVs were evident at 72 h post infection (hpi), including cell clustering, rounding, reticular structure formation, and a grape-like appearance (Fig. 1A, 1B). The negative control (NC) exhibited no such changes (Fig. 1C). Furthermore, transmission electron microscopy (TEM) analysis revealed the

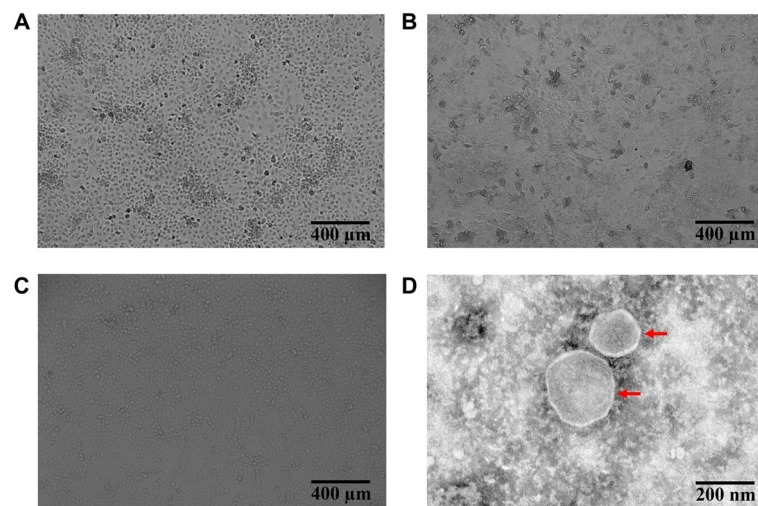


Fig. 1 Cytopathic effects of GTPV, LSDV, and the negative control, as well as the morphology of LSDV viral particles, were observed via TEM. **A** CPE of Vero cell sheets infected with GTPV. **B** CPE of Vero cell sheets infected with LSDV. **C** Uninfected Vero cell sheets observed for comparison. **D** TEM image of LSDV showing mature and immature viral particles indicated by arrows

characteristic brick-shaped virions of LSDV, measuring approximately 240–290 nm in diameter (Fig. 1D).

Detection of LSDV replication by PCR and qPCR

The 7th passage of LSDV cultured in Vero cells was sampled at five time points (24, 48, 72, 96, and 120 hpi) to monitor viral replication dynamics. LSDV viral nucleic acids were extracted and detected via PCR. The results revealed that the PCR products were of the expected size, with a gradual increase in band intensity over time (Fig. 2). These findings suggest active viral replication and highlight the temporal dynamics of LSDV propagation in Vero cells.

qPCR analysis targeting the *LSDV132* gene was performed on viral nucleic acids extracted from culture samples collected at five time points (24, 48, 72, 96 and 120 hpi). The results revealed that the copy number of the target fragment increased with time from 24–120 hpi (Fig. 3A). The peak copy number (log10) was observed at 96 hpi and was quantified *via* the standard curve equation $y = -0.253x + 11.611$ (Fig. 3B). To serve as a positive control, nucleic acid was extracted from Vero cells infected with GTPV AV41 at 24 hpi. The copy number was comparable to that of LSDV-infected cells at the same time point, confirming the reliability of the assay.

Indirect immunofluorescence assay

Vero cells infected with LSDV were examined at 72 hpi to assess fluorescence signaling. The results revealed that LSDV-infected cells displayed distinct and bright green fluorescence, indicating successful binding of the antibodies to the LSDV viral antigens. In contrast, cells in the

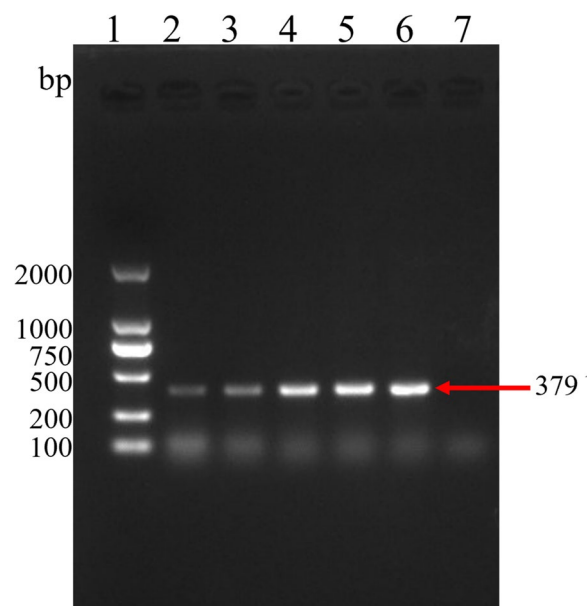


Fig. 2 Identification of LSDV nucleic acid via PCR. Lane 1: DL2000 ladder; Lanes 2–6: LSDV nucleic acids from different periods (24–120 hpi); Lane 7: Negative control

negative control group (uninfected Vero cells) showed no fluorescence, confirming the specificity of the assay. Similarly, positive control cells infected with GTPV presented bright green fluorescence (Fig. 4).

Phylogenetic analysis

The results of the comparison of whole-genome nucleotide sequences revealed that the nucleotide similarity

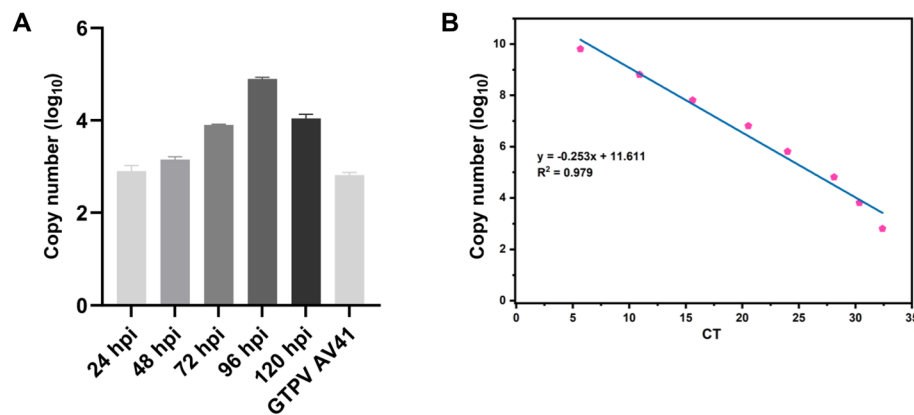


Fig. 3 Replication of LSDV was detected by qPCR. **A** Detection of LSDV viral proliferation (24–120 hpi) via qPCR; the nucleic acid extracted from Vero cells infected with GTPV AV41 at 24 hpi was used as the positive control. **B** A standard curve was plotted for the calculation of virus copy numbers at different time points. The X-axis represents the cycle threshold (CT), and the Y-axis represents the copy number (log₁₀)

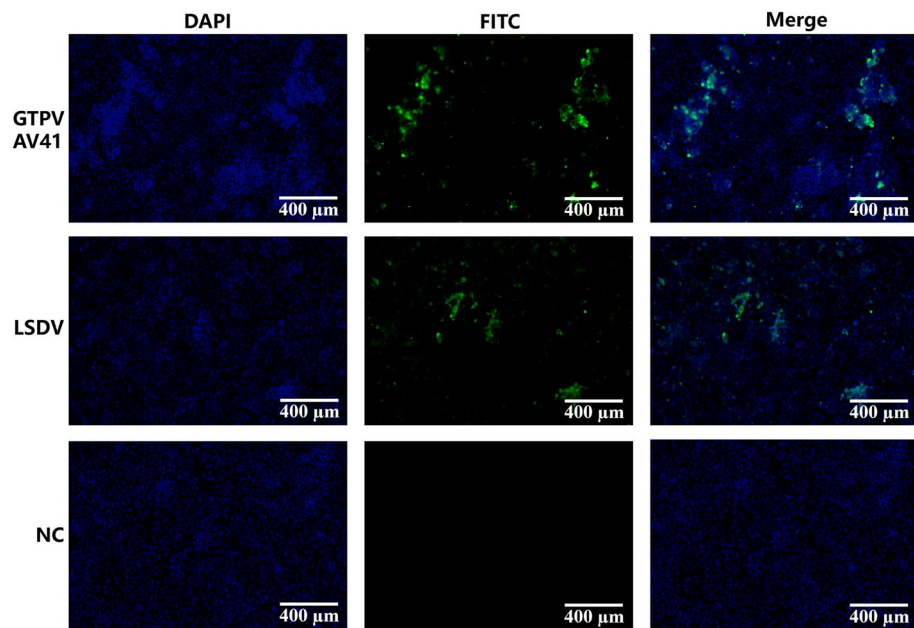


Fig. 4 Results of the indirect immunofluorescence assay. Both the positive control goatpox virus (GTPV) and the isolated LSDV/China/HB01/2020 strain reacted with positive sera specific to LSDV, resulting in bright green fluorescence. Additionally, negative uninfected Vero cells showed no fluorescence. Blue fluorescence (DAPI) was used to stain the nuclei, whereas green fluorescence (FITC-labeled anti-bovine IgG) was used to indicate specific binding of pAbs to LSDV. Merged images demonstrated the colocalization of viral antigens (green) within the cytoplasmic regions of infected cells. The primary antibody was serum from naturally LSDV-infected cattle

among 123 LSDV strains from 22 countries in southern Africa, Europe and Asia was as high as 98.4%–100%, indicating that the strains were closely related (Fig. 5A).

Phylogenetic analysis revealed that these 123 LSDV strains clustered into two major clades. The first major clade predominantly comprised isolates from African regions such as Kenya and Morocco; European regions such as Greece, Bulgaria, and Albania; and Asian regions such as India and Bangladesh. These

strains showed a high degree of clustering, indicating close genetic relatedness. In contrast, the second major clade presented greater genetic diversity and was further subdivided into two subclades. Subclade 1 primarily included LSDV vaccine-recombinant strains prevalent in Asian countries, including China, Vietnam, Malaysia, Thailand, and Indonesia. Subclade 2 mainly consisted of wild-type and vaccine strains circulating in African regions. Notably, the LSDV/

CHINA/Tibet/2023 isolate clustered with six Indian isolates, suggesting regional grouping and a close genetic relationship despite belonging to distinct evolutionary branches (Fig. 5B). These clustering patterns likely reflected the virus's transmission history and evolutionary dynamics across different geographical regions.

Furthermore, recombination events among LSDV strains were analyzed to gain insight into the evolutionary origins of the virus, which is critical for developing effective prevention and control strategies. A total of 123 complete LSDV genomes were retrieved from the NCBI database and analyzed *via* Geneious software. Recombination analysis was performed with the RDP 4 program, which identified 70 recombination events (Supplementary Table 10). Notably, LSDV/China/Xinjiang/Cattle/Aug-2019 had the Bangladesh LSD vaccine and V281/Nigeria as major parental strains, with LSD-148-GP-RSA-1997 serving as the minor parent (Supplementary Table 11). Similarly, LSDV/HongKong/2020 shares the Bangladesh LSD vaccine strain, V281/Nigeria, and LSDV/Kurgan/2018 as major parental strains, with LSD-148-GP-RSA-1997 again identified as the minor parent (Supplementary Table 12). These findings were further validated through similarity plot analyses (Supplementary Figs. 2–6).

Sequencing and analysis of the *LSDV011* gene in LSDV/China/HB01/2020

First, three genes, namely, *LSDV011*, *LSDV035*, and *LSDV074* were amplified and subsequently cloned into the pMD-19 T vector to obtain their nucleotide sequences by Sanger sequencing (Fig. 6A). After retrieving and downloading the complete genome sequences of 123 LSDV strains from the NCBI database, we excluded those lacking annotations for the *LSDV011* gene and performed multiple sequence alignment of the *LSDV011* gene from the remaining 118 strains *via* Geneious software. Sequence analysis of LSDV/China/HB01/2020 revealed 96.9%–100% nucleotide similarity with the other 117 LSDV strains. Further phylogenetic analysis of the *LSDV011* gene revealed that LSDV/China/HB01/2020 clustered within the same evolutionary clade as 15 other Chinese isolates did, which was consistent with the results obtained from the whole-genome phylogenetic

analysis (Fig. 6B). Notably, several strains within this clade had previously been confirmed as recombinant viruses, suggesting a potential role of recombination in the evolution of LSDV in China.

Recombination analysis of isolated LSDV/China/HB01/2020

To investigate the evolutionary origin of LSDV and provide a theoretical basis for clinical prevention and control strategies, we conducted multiple sequence alignment of the *LSDV011* gene from LSDV/China/HB01/2020 with those of 117 other representative LSDV strains via Geneious software. Recombination analysis via the RDP 4 program indicated a potential recombination event in the *LSDV011* gene of LSDV/China/HB01/2020 (Table 1). The analysis suggested that V395.1/Bangladesh and LSDV/Russia/Tyumen/2019 likely served as parental strains. Furthermore, similarity plot analysis confirmed the presence of two genomic exchange regions within the *LSDV011* gene of LSDV/China/HB01/2020, located at positions 120 nt and 762 nt (Fig. 6C).

Recombination analysis between the GTPV and LSDV

To explore potential genetic recombination events between wild-type LSDV strains and attenuated GTPV vaccine strains, we retrieved the complete genome sequences of 13 GTPV isolates from the NCBI database and selected 65 LSDV isolates from various Asian regions. We performed multiple sequence alignment of these 78 viral genomes using Geneious software. Subsequently, recombination analyses were conducted via RDP 4, a tool specifically designed to detect recombination in viral genomes. The analysis revealed two distinct recombination events between GTPV and LSDV strains isolated in Asia (Table 2). Notably, RDP 4 indicated that the goatpox virus isolate Turkey had goatpox virus isolate Vietnam as its major parent and goatpox virus V103 as its minor parent. Similarly, it identified the goatpox virus isolate Yemen as the major parent of LSDV/2021/Banswara, with China/Xinjiang/Cattle/Aug-2019 serving as the minor parent. These results were further validated via similarity plot analyses (Supplementary Figs. 7 and 8). Importantly, none of these recombination events involved the GTPV AV41 vaccine strain. This recombination could lead to the emergence of novel viral strains with unique biological characteristics.

(See figure on next page.)

Fig. 5 Phylogenetic analysis of the complete genome sequences of 123 LSDV strains. **A** Nucleotide similarity among 123 LSDV strains originating from 22 countries in South Africa, Europe, and Asia ranged from 98.4%–100%. **B** Phylogenetic analysis revealed that 123 LSDV strains from 22 countries were grouped into two primary clades. Blue, green, and pink represent one of the primary clades, with strains originating mainly from Africa, Europe, and certain Asian countries (India and Bangladesh). Yellow represents wild-type and vaccine strains prevalent in Africa. Red represents vaccine-recombinant strains that circulated in Asia

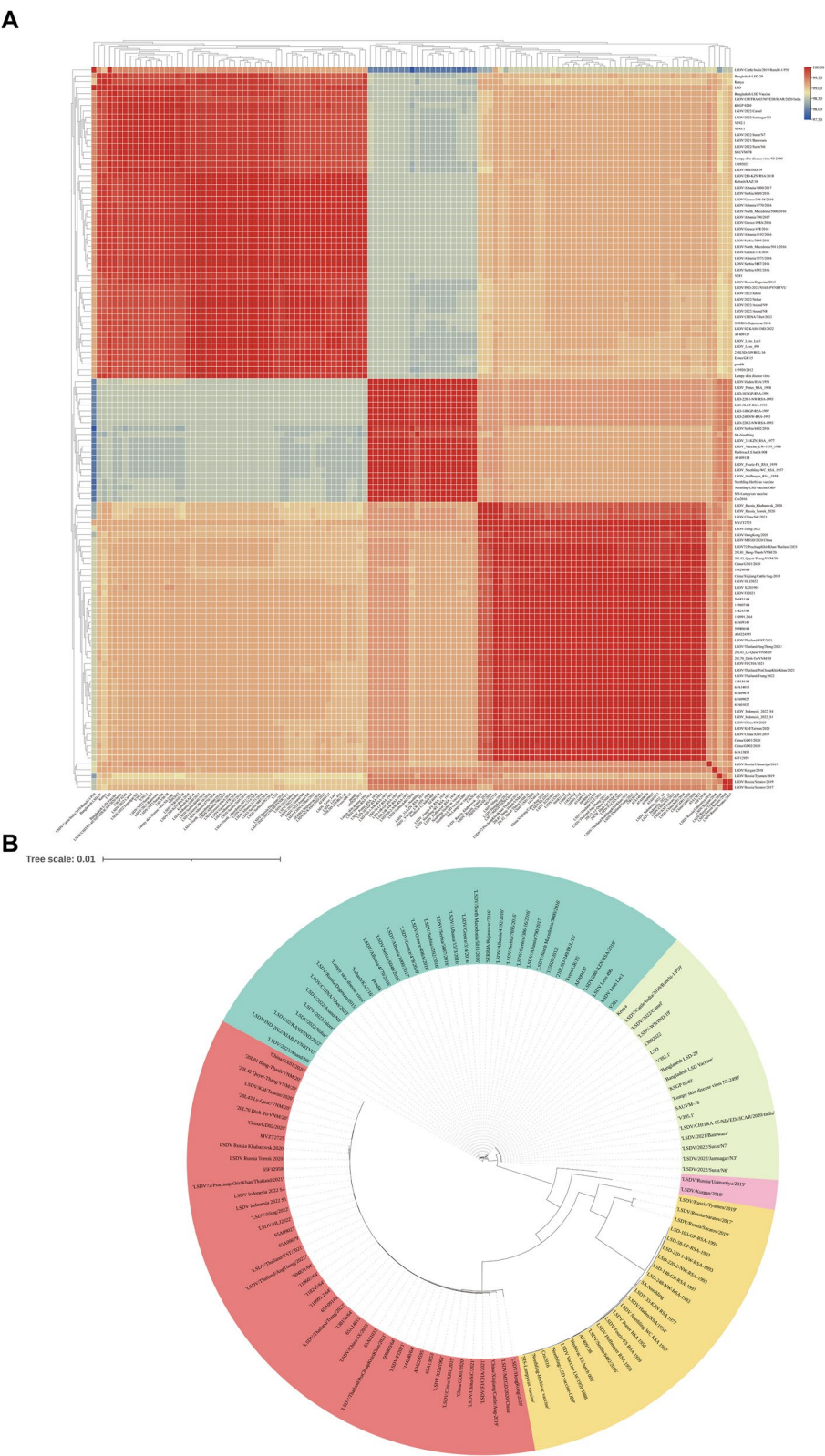


Fig. 5 (See legend on previous page.)

Discussion

LSDV isolation was conducted under strict biosafety protocols using Vero cells, which are highly sensitive to the CaPV genus and suitable for poxvirus isolation and propagation (Rhazi et al. 2021; Kumar et al. 2021).

Owing to the large size of poxviruses, measuring approximately (294 ± 20) nm in length and (262 ± 22) nm in width, we used a $0.45 \mu\text{m}$ filter to process the supernatant from homogenized positive tissue samples (Akther et al. 2023; Wang et al. 2022). To mitigate bacterial contamination, antibiotics were added to a final concentration of 5% during sample processing before the supernatant was inoculated into Vero cells. The LSDV/China/HB01/2020 isolate was confirmed by PCR and qPCR to target the conserved *LSDV132* gene, followed by sequence analysis. qPCR demonstrated effective virus replication in Vero cells, with a strong correlation ($R^2 = 0.9795$) and an amplification efficiency of 82.1%, which was slightly below the ideal range, indicating that the qPCR system could be further optimized. Furthermore, the peak viral nucleic acid value of LSDV propagated in Vero cells was consistent with the findings reported by Zhou et al. (Zhou et al. 2024). In their study, LSDV was detected by PCR in samples from three provinces in China and was successfully isolated from primary lamb testicular cells (PLTs) in 2022, with a high viral titer observed at 96 hpi.

Genomic and phylogenetic analyses revealed high genetic similarity (98.4%–100%) among LSDV strains from various geographical regions, with distinct regional clustering patterns. These strains can be divided into three main regions: Asia, Europe and Africa. The *LSDV011*, *LSDV035*, and *LSDV074* genes, which encode the GPCR, RPO30, and P32 proteins, respectively, have frequently been used in genetic evolution analyses of LSDV (Sprygin et al. 2020; Zaghloul et al. 2022). Notably, recombination events within the *LSDV011* gene of the LSDV/China/HB01/2020 strain highlighted its evolutionary adaptability and potential for interregional genetic exchange. In contrast, recombination analyses of the *LSDV035* and *LSDV074* genes in the same isolate revealed no detectable recombination events. However, a K-to-N amino acid mutation and a distinctive amino acid insertion at the L position were identified in the

LSDV035 gene. Since 2017, the emergence of recombinant LSDVs in Russia, Kazakhstan, China and Vietnam has led to additional distinct clusters (Krotova et al. 2022). It is now thought that the contaminated Lumpivax vaccine gave rise to recombinant vaccine-like LSDV strains in Asia (Vandenbussche et al. 2022). Whole-genome sequencing and phylogenetic analysis of the isolate LSDV/MZGD/2020 revealed close relationships with Asian strains, forming a new clade. RDP 4, Simplot, and phylogenetic analyses confirmed that this isolate was a vaccine-like recombinant strain, reinforcing the idea that Chinese LSDV strains are vaccine-derived recombinants (Wang et al. 2022). Other studies have suggested that LSDV outbreaks have occurred in Thailand since 2021, with strains sharing 99.8%–100% similarity with isolates from Russia, India, and Kenya (Arjkumpa et al. 2021). Additionally, an LSDV strain (OR797612.1) isolated from yaks on the Tibetan Plateau, China, in 2023 exhibited high similarity to a 2022 Indian isolate, highlighting the increasing risk of LSDV recombination (Song et al. 2024). There is a growing body of evidence that recombination in DNA viruses not only is readily possible but can also generate hybrid progeny in the field, causing disease (Lee et al. 2012). Russia began using attenuated SPPV vaccines to control LSD outbreaks in 2016; however, multiple incursions of vaccine-like strains have occurred since 2017 (Sprygin et al. 2018a, 2018b). When the live attenuated LSDV vaccine was being administered in Kazakhstan, it borders Kazakhstan (Kononov et al. 2019a, b). In the same year, a naturally occurring recombinant vaccine, Saratov/2017, was first isolated from the same geographic region (Sprygin et al. 2018a, b, c). In our study, we confirmed potential recombination events between LSDV and GTPV, although no recombination involving the GTPV AV41 vaccine strain was detected. These findings underscore the importance of developing safer LSDV vaccines to prevent the emergence of recombinant strains (Whittle et al. 2023).

To distinguish between the wild-type and vaccine-derived LSDV strains, the *LSDV126* gene of the LSDV/China/HB01/2020 strain was analyzed. Sequencing revealed 100% homology with the China/GD01/2020 strain. Phylogenetic analysis further confirmed that it clustered with vaccine-like recombinant strains from

(See figure on next page.)

Fig. 6 Phylogenetic and similarity plot analysis of the nucleotide sequence of the *LSDV011* gene. **A** 1: DL2000 ladder; 2: *LSDV011* gene; 3: *LSDV035* gene; 4: *LSDV074* gene; 5: Negative control. **B** Phylogenetic analysis was performed on 118 LSDV isolates, including LSDV/China/HB01/2020, on the basis of the *LSDV011* gene. Green: Wild-type LSDV strains from Africa; yellow: LSDV isolates from Europe; purple/red: LSDV isolates from Asia. **C** Similarity plot analysis identified two genomic exchange regions within the *LSDV011* gene of LSDV/China/HB01/2020 at positions 120 nt and 762 nt. X-axis: nucleotide sequence position; Y-axis: nucleotide sequence similarity; Red: the primary parent was LSDV/Russia/Tyumen/2019; Green: the secondary parent was V395.1/Bangladesh

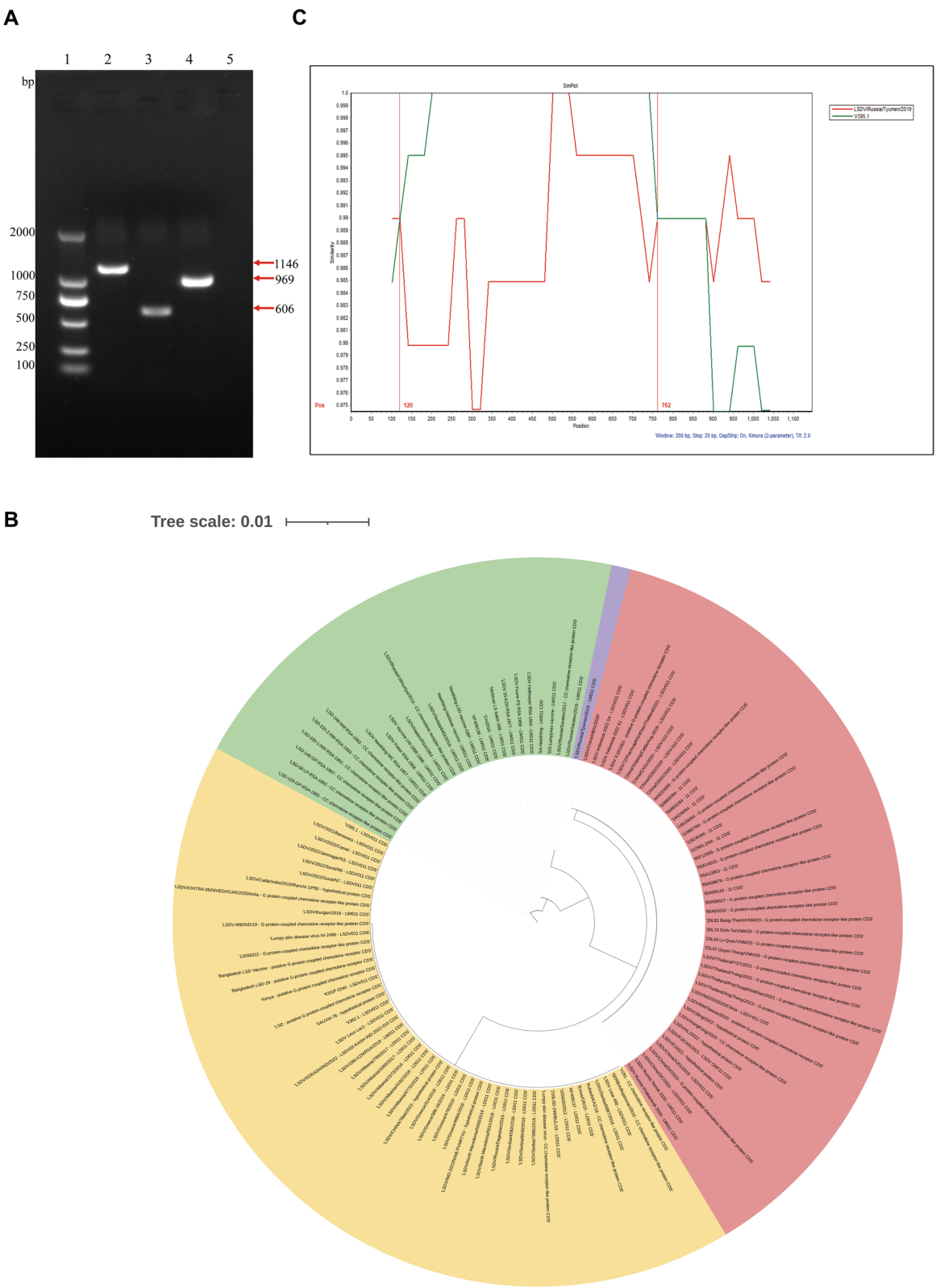


Fig. 6 (See legend on previous page.)

Table 1 RDP 4 program to analyze the *LSDV011* gene recombination events of LSDV strains

Recombination	Event 1	
Strains	LSDV/China/HB01/2020	
Beginning breakpoint	120	
Ending breakpoint	836	
Major parent	V395.1/Bangladesh	
Minor parent	LSDV/Russia/Tyumen/2019	
Methods (p Value)	RDP	/
	GENECONV	/
	Chimera	1.052×10^{-02}
	MaxChi	5.833×10^{-03}
	BootScan	/
	SiScan	/
	3Seq	1.644×10^{-03}

Russia, Thailand, and Vietnam, supporting the hypothesis of cross-border transmission. Retrospective studies have also demonstrated that LSDV strains in China, such as LSDV/China/XJ01/2019 and LSDV/China/GD01/2020, share 100% nucleotide sequence identity across 150 open reading frames (ORFs) with 97.1%–99.7% similarity in six other ORFs, indicating a common ancestral origin with vaccine-like strains (Wei et al. 2023).

Effective control of LSDV requires a multifaceted approach, including international cooperation to regulate cross-border animal trade, strict quarantine measures, and vector control targeting blood-feeding insects such as *Aedes aegypti* and *Stomoxys calcitrans* (Saegerman et al. 2018; Azeem et al. 2022). Continuous monitoring of LSDV evolution, along with the development of highly effective vaccines and diagnostic tools, is essential for eradicating the disease and promoting sustainable livestock farming in China.

Conclusions

In conclusion, this study successfully isolated the LSDV/China/HB01/2020 strain from clinical skin tissue samples of diseased beef cattle in Hubei Province, China. Furthermore, we confirmed its evolutionary relationship with other Asian strains, identified recombination events, and highlighted the urgent need for novel, safer vaccines to control LSD in the cattle industry.

Methods

Cells, serum samples, and viruses

Vero cells were stored in our laboratory. Serum samples were obtained from naturally infected cattle on a farm with an LSD outbreak, which was confirmed by PCR of the *LSDV132* gene and sequencing of the PCR product in this study. All the serum samples were confirmed as LSDV-positive by both the ID Screen® Capripox Double Antigen ELISA Kit (ID-vet, Grabels, France) and the virus neutralization test (VNT) performed in this study. These LSDV-positive sera were used in subsequent immunofluorescence assay (IFA) experiments. The live attenuated goatpox vaccine strain (GTPV AV41) was obtained for use in VNT from Jilin Zhengye Biological Co., Ltd.

Virus isolation and electron microscope observation

Tissue samples suspected of LSDV infection, including clinical skin nodule tissues from diseased beef cattle, were collected from a farm in Hubei Province, China, and transported to the ABSL-3 laboratory at Huazhong Agricultural University. Virus isolation was performed as previously described (Zhang et al. 2020). The samples were finely diced and transferred to 1.5 mL EP tubes containing three sterile grinding beads. A mixture of DMEM (Thermo, Gibco, USA) and 5% penicillin–streptomycin solution (Thermo, Gibco, USA) was added at a 1:2 ratio to tissue volume. The samples were homogenized using a

Table 2 RDP 4 program to analyze the recombination events of LSDV and GTPV strains isolated from Asia

Recombination	Event 1		Event 2
Strains	Goatpox virus isolate Turkey		LSDV/2021/Banswara
Beginning breakpoint	538		5407
Ending breakpoint	151,748		6369
Major parent	Goatpox virus isolate Vietnam		Goatpox virus isolate Yemen
Minor parent	Goatpox virus V103		China/Xinjiang/Cattle/Aug-2019
Methods (p Value)	RDP	8.594×10^{-29}	3.941×10^{-26}
	GENECONV	3.229×10^{-16}	2.869×10^{-18}
	Chimera	1.617×10^{-08}	6.256×10^{-11}
	MaxChi	1.901×10^{-08}	1.910×10^{-10}
	BootScan	5.471×10^{-28}	3.552×10^{-22}
	SiScan	/	/
	3Seq	3.079×10^{-12}	3.151×10^{-13}

mechanical tissue grinder and subsequently centrifuged at $4000 \times g$ for 15 min. The supernatant was filtered through a $0.45 \mu\text{m}$ membrane filter (Merck, Millipore, Germany) and used to inoculate Vero cells at 70%–80% confluence in 6-well plates containing DMEM with 5% FBS (Qingmu, Wuhan, China) and 2% penicillin–streptomycin solution. After incubation at 37°C with 5% CO_2 for 2 h, the inoculum was removed, and the cells were washed three times with PBS. Cells were then maintained in DMEM containing 2% FBS and 1% penicillin–streptomycin until the CPEs were observed. The plates subsequently underwent three freeze–thaw cycles at -80°C . The lysate was centrifuged at $4000 \times g$ for 10–15 min, and the virus-containing supernatant was stored at -80°C for further use.

For virus amplification, the supernatant was inoculated into Vero cell monolayers in T175 flasks and cultured in DMEM maintenance medium at 37°C with 5% CO_2 for 5 d. After incubation, cells underwent three freeze–thaw cycles at -80°C . The culture supernatant was collected, centrifuged at $4000 \times g$ for 10–15 min at 4°C to remove cellular debris, and further purified by ultracentrifugation. Viral particles were then sent to Wuhan Servicebio Technology Co., Ltd. for observation by transmission electron microscopy (TEM).

Detection of LSDV replication by PCR and qPCR

At 24, 48, 72, 96, and 120 hpi, viral nucleic acid was extracted from the cell culture supernatant via a viral DNA extraction kit specific for LSDV (Tianmo, Beijing, China). PCR targeting the *LSDV132* gene was performed according to the Lumpy Skin Disease diagnostic standard GB/T 39602–2020 (Supplementary Tables 1 and 2). The primers were synthesized to amplify a 379 bp fragment. The PCR conditions were as follows: initial denaturation at 94°C for 5 min; 35 cycles at 94°C for 30 s, 54°C for 30 s, and 72°C for 30 s; a final extension at 72°C for 10 min; and storage at 4°C . The PCR products were analyzed *via* 1% agarose electrophoresis and sent for sequencing to Wuhan Tsingke Biotechnology Co., Ltd.

To evaluate LSDV proliferation in Vero cells, 500 μL of the seventh passage LSDV suspension was diluted to 1 mL with serum-free DMEM and added to Vero cell monolayers at 70%–80% confluency in a T25 flask. The flask was incubated at 37°C for 2 h to allow viral adsorption. After incubation, the inoculum was removed, and 5 mL of maintenance medium was added. The cultures were maintained at 37°C with 5% CO_2 , and the supernatants were collected every 24 h over a 5-day period. The collected supernatants were subjected to three freeze–thaw cycles and centrifuged at $4000 \times g$ for 15 min to remove cellular debris. A qPCR assay targeting the *LSDV132* gene was designed to amplify a 135 bp

fragment and was used to evaluate LSDV proliferation in Vero cells (Supplementary Tables 3 and 4).

Indirect immunofluorescence assay

Indirect immunofluorescence assay was performed as previously described (Zhang et al. 2020). Vero cells were seeded in six-well plates and cultured to 70%–80% confluence. Monolayers were infected with LSDV at a multiplicity of infection (MOI) of 0.1 and incubated at 37°C for 2 h to allow viral adsorption. After removing the inoculum, cells were washed with PBS, and incubated for 72 hpi. Cells were fixed with 4% paraformaldehyde (Beyotime, Shanghai, China) for 15 min at 25°C , washed with PBS, permeabilized with 1% Triton X-100 (Beyotime) for 10 min, and blocked with 5% bovine serum albumin (BSA) (Merck, Sigma, USA) for 1 h at 25°C . LSDV-positive cattle serum diluted 1:50 in PBS was added and incubated at 37°C for 1 h. After washing, FITC-conjugated rabbit anti-bovine IgG (H+L) (Biodragon, Beijing, China), diluted 1:250 in PBS, was added as the secondary antibody and incubated in the dark at 37°C for 1 h. Cells were then washed three times with PBS in the dark and stained with 500 μL of DAPI solution (Beyotime, Shanghai, China) for 10 min at 25°C . Finally, the cells were washed and maintained in 500 μL of PBS. Fluorescence images were acquired using a fluorescence microscope (Thermo Fisher, Waltham, USA).

Gene sequencing and phylogenetic analysis

To systematically characterize the genetic features of LSDV, whole-genome sequences of 123 strains were retrieved from GenBank. Multiple sequence alignment and phylogenetic analysis were performed using Geneious Prime software (2023.0.3). Potential recombination events were assessed using RDP4 (v4.101) with seven algorithms (RDP, GENECONV, Chimaera, MaxChi, BootScan, SiScan, and 3Seq), and only events supported by at least three of these methods ($p < 0.05$) were considered reliable (Martin et al. 2005; Posada & Crandall 2001). Simplot (V. 3.5.1) was used for the visualization analysis of the recombination events (Xu et al. 2024).

To further analyze the LSDV/China/HB01/2020 isolate, three genes (*LSDV011*, *LSDV035*, and *LSDV074*) were amplified and cloned into the pMD-19 T vector (Takara, Beijing, China) *via* TA cloning. Positive clones were confirmed using M13-F/R primers, and the verified products were sequenced by Wuhan Tsingke Biotechnology Co., Ltd. PCR amplification was performed using $2\times$ Phanta Flash Master Mix (Vazyme, Nanjing, China) under standard thermal cycling conditions: initial denaturation at 98°C for 30 s, followed by 35 cycles of denaturation at 98°C for 10 s, annealing at 50°C for 5 s, and extension at 72°C for 10 s. A final extension was conducted at 72°C for

1 min, and the products were stored at 4°C. The specific primers and reaction components are provided in Supplementary Tables 5 and 6. Colony PCR identification was conducted with 2× Rapid Taq Master Mix (Vazyme, Nanjing, China) under the following conditions: initial denaturation at 95°C for 5 min, followed by 35 cycles of denaturation at 95°C for 15 s, annealing at 54°C for 15 s, and extension at 72°C for 30 s. A final extension was performed at 72°C for 5 min, and the products were stored at 4°C. The specific primers and reaction conditions are shown in Supplementary Tables 7 and 8. The nucleotide sequences of the *LSDV011*, *LSDV035*, and *LSDV074* genes from the LSDV/China/HB01/2020 isolate were submitted to GenBank under accession numbers PQ852094, PQ852095, and PQ852096, respectively. Phylogenetic and amino acid sequence analyses were performed to compare these genes with reference strains, as detailed in Supplementary Table 9.

Abbreviations

LSD	Lumpy skin disease
LSDV	Lumpy skin disease virus
CaPVs	Capripox virus
CPEs	Cytopathic effects
QPCR	Quantitative PCR
TEM	Transmission electron microscopy
IFA	Indirect immunofluorescence assay
GTPV	Goatpox virus
WOAH	World Organization for Animal Health
NC	Negative control
PLT	Primary lamb testicular
ORFs	Open reading frames
VNT	Virus neutralization test
Hpi	Hours post infection
MOI	Multiplicity of infection

Supplementary Information

The online version contains supplementary material available at <https://doi.org/10.1186/s44149-025-00182-x>.

Supplementary Material 1: Table S1 List of PCR primers used in this study. Table S2 Amplification system for PCR. Table S3 List of qPCR primers used in this study. Table S4 Amplification system for qPCR. Table S5 List of PCR primers used in this study. Table S6 Amplification system for PCR. Table S7 List of PCR primers used in this study. Table S8 PCR identification system. Table S9 Reference strains used for the phylogenetic analysis of LSDV in this study. Table S10 RDP 4 program for analyzing the genomic recombination events of LSDV strains. Table S11 RDP 4 program to analyze the recombination events of LSDV/China/Xinjiang/Cattle/Aug-2019. Table S12 RDP 4 program to analyze the recombination events of LSDV/HongKong/2020. Fig. S1 PCR identification of LSDV nucleic acid. (A) Lane 1: DL2000 ladder; Lanes 2–5: Clinical samples; Lane 6: Positive control; Lane 7: Negative control. (B) Results of nucleotide alignment of the *LSDV132* gene via Sanger sequencing. Fig. S2 Recombination analysis of the LSDV/China/Xinjiang/Cattle/Aug-2019 strains. The primary parental isolate of China/Xinjiang/Cattle/Aug-2019 was the Bangladesh LSD vaccine, with LSD-148-GP-RSA-1997 serving as the secondary parental isolate. The X-axis represents the nucleotide sequence position, and the Y-axis represents the nucleotide sequence similarity. Orange represents that the primary parent is the Bangladesh LSD vaccine. Purple represents that the secondary parent is LSD-148-GP-RSA-1997. Fig. S3 Recombination analysis of the LSDV/China/Xinjiang/Cattle/Aug-2019 strains. The primary parental isolate of China/Xinjiang/Cattle/Aug-2019 was V281/Nigeria,

with LSD-148-GP-RSA-1997 serving as the secondary parental isolate. The X-axis represents the nucleotide sequence position, and the Y-axis represents the nucleotide sequence similarity; red represents the primary parent V281/Nigeria; purple represents the secondary parent LSD-148-GP-RSA-1997. Fig. S4 Recombination analysis of the LSDV/HongKong/2020 strain. The primary parental isolate of the LSDV/HongKong/2020 strain was the Bangladesh LSD vaccine, with LSD-148-GP-RSA-1997 serving as the secondary parental isolate. The X-axis represents the nucleotide sequence position, and the Y-axis represents the nucleotide sequence similarity. Green represents the following: the primary parent is the Bangladesh LSD vaccine; purple represents the secondary parent LSD-148-GP-RSA-1997. Fig. S5 Recombination analysis of the LSDV/HongKong/2020 strain. The primary parental isolate of LSDV/HongKong/2020 was V281/Nigeria, with LSD-148-GP-RSA-1997 serving as the secondary parental isolate. The X-axis represents the nucleotide sequence position, and the Y-axis represents the nucleotide sequence similarity. Dark green represents the following: the primary parent was V281/Nigeria; purple represents the secondary parent LSD-148-GP-RSA-1997. Fig. 6 Recombination analysis of the LSDV/HongKong/2020 strain. The primary parental isolate of LSDV/HongKong/2020 was LSDV/Kurgan/2018, with LSD-148-GP-RSA-1997 serving as the secondary parental isolate. The X-axis represents the nucleotide sequence position, and the Y-axis represents the nucleotide sequence similarity. Black represents the following: the primary parent is LSDV/Kurgan/2018; purple represents the secondary parent LSD-148-GP-RSA-1997. Fig. S7 Recombination analysis of the Goatpox virus Turkey strain. The primary parental isolate of the Goatpox virus from Turkey was the Goatpox virus isolate from Vietnam, with Goatpox virus V103 serving as the secondary parental isolate. The X-axis represents the nucleotide sequence position, and the Y-axis represents the nucleotide sequence similarity. Pink represents the following: the primary parent was the Goatpox virus isolate from Vietnam; blue represents the secondary parent, which was Goatpox virus V103. Fig. S8 Recombination analysis of the LSDV/2021/Banswara strain. The primary parental isolate of LSDV/2021/Banswara was identified as the Goatpox virus isolate from Yemen, with China/Xinjiang/Cattle/Aug-2019 serving as the secondary parental isolate. The X-axis represents the nucleotide sequence position, and the Y-axis represents the nucleotide sequence similarity. Blue represents the primary parent, which was the Goatpox virus isolate from Yemen; red represents the secondary parent, which was China/Xinjiang/Cattle/Aug-2019.

Acknowledgements

The authors gratefully acknowledge the funding support.

Authors' contributions

A.Z.G. and C.M.H. conceived and designed the experiments; X.W.Y., X.W.X., Q.N.L., C.W., and Z.J.X. performed the experiments and analyzed the data; X.W.Y. wrote the manuscript. A.Z.G., C.M.H. and Y.Y.C. checked and finalized the manuscript. All the authors have read and approved the final version of the manuscript.

Funding

This work was financially supported by the National Key Research and Development Program of China (#2023YFD1802505), the National Key Research and Development Program of China (#2022YFD1800701), and the Chinese Agricultural Research System of MOF and MARA (#CARS-37).

Data availability

The data supporting the findings of this study are available within the article, and further inquiries can be directed to the corresponding author.

Declarations

Ethics approval and consent to participate

This study was conducted in strict accordance with the recommendations provided in the Guide for the Care and Use of Laboratory Animals of the Ministry of Science and Technology of the People's Republic of China. The animal experiments were approved by the Hubei Administrative Committee for Laboratory Animals (Approval No. HZAUCA-2023-0022).

Consent for publication

All the authors approved and provided their consent for publication of the manuscript.

Competing interests

The authors declare that they have no competing interests.

Author details

¹National Key Laboratory of Agricultural Microbiology, College of Veterinary Medicine, Hubei Hongshan Laboratory, Huazhong Agricultural University, Wuhan 430070, China. ²Cooperative Innovation Center for Sustainable Pig Production, Huazhong Agricultural University, Wuhan 430070, China. ³Hubei International Scientific and Technological Cooperation Base of Veterinary Epidemiology, Wuhan 430070, China.

Received: 9 April 2025 Accepted: 10 June 2025

Published online: 27 June 2025

References

- Abeba, B. 2024. Prevalence of lumpy skin disease in Africa: A systematic review and meta-analysis from 2007 to 2023. *Veterinary Medicine International*. 2024:9991106. <https://doi.org/10.1155/2024/9991106>.
- Abutarbush, S. M., M. M. Ababneh, I. G. Al Zoubi, O. M. Al Sheyab, M. G. Al Zoubi, M. O. Aleksh, and R. J. Al Gharabat. 2015. Lumpy skin disease in Jordan: Disease emergence, clinical signs, complications and preliminary-associated economic losses. *Transboundary and Emerging Diseases* 62 (5): 549–554. <https://doi.org/10.1111/tbed.12177>.
- Akther, M., S. H. Akter, S. Sarker, J. W. Aleri, H. Annandale, S. Abraham, and J. M. Uddin. 2023. Global burden of lumpy skin disease, outbreaks, and future challenges. *Viruses* 15 (9): 1861. <https://doi.org/10.3390/v15091861>.
- Annandale, C. H., D. E. Holm, K. Ebersohn, and E. H. Venter. 2014. Seminal transmission of lumpy skin disease virus in heifers. *Transboundary and Emerging Diseases* 61 (5): 443–448. <https://doi.org/10.1111/tbed.12045>.
- Arijkuma, O., M. Suwannaboon, M. Boonrawd, I. Punyawan, P. Laobannu, S. Yantaphan, A. Bungwai, V. Ponyium, N. Suwankitwat, P. Boonpornprasert, et al. 2021. First emergence of lumpy skin disease in cattle in Thailand, 2021. *Transboundary and Emerging Diseases* 68 (6): 3002–3004. <https://doi.org/10.1111/tbed.14246>.
- Azeem, S., Sharma B, Shabir S, Akbar H, Venter E. 2022. Lumpy skin disease is expanding its geographic range: A challenge for Asian livestock management and food security. *Veterinary journal (London, England: 1997)* 279: 105785. <https://doi.org/10.1016/j.tvjl.2021.105785>.
- Badhy, S. C., M. G. A. Chowdhury, T. B. K. Settypalli, G. Cattoli, C. E. Lamien, M. A. U. Fakir, S. Akter, M. G. Osmani, F. Talukdar, N. Begum, I. A. Khan, M. B. Rashid, and M. Sadekuzzaman. 2021. Molecular characterization of lumpy skin disease virus (LSDV) emerged in Bangladesh reveals unique genetic features compared to contemporary field strains. *BMC Veterinary Research* 17 (1): 61. <https://doi.org/10.1186/s12917-021-02751-x>.
- Chihota, C. M., L. F. Rennie, R. P. Kitching, and P. S. Mellor. 2003. Attempted mechanical transmission of lumpy skin disease virus by biting insects. *Medical and Veterinary Entomology* 17 (3): 294–300. <https://doi.org/10.1046/j.1365-2915.2003.00445.x>.
- European Food Safety Authority (EFSA); Calistri P, De Clercq K, Gubbins S, Klement E, Stegeman A, Cortiñas Abrahantes J, Marojevic D, Antoniou SE, Broglia A 2020 Lumpy skin disease epidemiological report IV: Data collection and analysis EFSA Journal. European Food Safety Authority 18 2 e06010 <https://doi.org/10.2903/j.efsa.2020.6010>
- Di Giuseppe A, Zenobio V, Dall'Acqua F, Di Sabatino D, Calistri P. 2024. Lumpy skin disease. *The Veterinary clinics of North America. Food animal practice* 40(2): 261–276. <https://doi.org/10.1016/j.cvfa.2024.01.002>.
- Haga, I. R., B. B. Shih, G. Tore, N. Polo, P. Ribeca, D. Gombo-Ochir, G. Shura, T. Tserenchim, B. Enkhbold, D. Purevtsuren, et al. 2024. Sequencing and analysis of lumpy skin disease virus whole genomes reveals a new viral subgroup in West and Central Africa. *Viruses* 16 (4): 557. <https://doi.org/10.3390/v16040557>.
- Hunter, P., and D. Wallace. 2001. Lumpy skin disease in southern Africa: A review of the disease and aspects of control. *Journal of the South African Veterinary Association* 72 (2): 68–71. <https://doi.org/10.4102/j.sava.v72i2.619>.
- Issimov, A., L. Kutumbetov, M. B. Orynbayev, B. Khairullin, B. Myrzakhmetova, K. Sultankulova, and P. J. White. 2020. Mechanical transmission of lumpy skin disease virus by *Stomoxys* Spp (*Stomoxys Calcitrans*, *Stomoxys Sittens*, *Stomoxys Indica*), Diptera: Muscidae. *Animals* 10 (3): 477. <https://doi.org/10.3390/ani10030477>.
- Klausner, Z., E. Fattal, and E. Klement. 2017. Using synoptic systems' typical wind trajectories for the analysis of potential atmospheric long-distance dispersal of lumpy skin disease virus. *Transboundary and Emerging Diseases* 64 (2): 398–410. <https://doi.org/10.1111/tbed.12378>.
- Kononov, A., O. Byadovskaya, S. Kononova, R. Yashin, N. Zinyakov, V. Mischenko, N. Perevozchikova, and A. Sprygin. 2019a. Detection of vaccine-like strains of lumpy skin disease virus in outbreaks in Russia in 2017. *Archives of Virology* 164 (6): 1575–1585. <https://doi.org/10.1007/s00705-019-04229-6>.
- Kononov, A., P. Prutnikov, I. Shumilova, S. Kononova, A. Nesterov, O. Byadovskaya, Y. Pestova, V. Diev, and A. Sprygin. 2019b. Determination of lumpy skin disease virus in bovine meat and offal products following experimental infection. *Transboundary and Emerging Diseases* 66 (3): 1332–1340. <https://doi.org/10.1111/tbed.13158>.
- Krotova, A., O. Byadovskaya, I. Shumilova, A. van Schalkwyk, and A. Sprygin. 2022. An in-depth bioinformatic analysis of the novel recombinant lumpy skin disease virus strains: From unique patterns to established lineage. *BMC Genomics* 23 (1): 396. <https://doi.org/10.1186/s12864-022-08639-w>.
- Kumar, N., Y. Chander, R. Kumar, N. Khandelwal, T. Riyesh, K. Chaudhary, K. Shanmugasundaram, S. Kumar, A. Kumar, M. K. Gupta, et al. 2021. Isolation and characterization of lumpy skin disease virus from cattle in India. *PLoS ONE* 16 (1): e0241022. <https://doi.org/10.1371/journal.pone.0241022>.
- Lee, S. W., P. F. Markham, M. J. Coppo, A. R. Legione, J. F. Markham, A. H. Noor-mohammadi, G. F. Browning, N. Ficorilli, C. A. Hartley, and J. M. Devlin. 2012. Attenuated vaccines can recombine to form virulent field viruses. *Science* 337 (6091): 188. <https://doi.org/10.1126/science.1217134>.
- Lubinga, J. C., E. S. Tuppurainen, W. H. Stoltz, K. Ebersohn, J. A. Coetzer, and E. H. Venter. 2013. Detection of lumpy skin disease virus in saliva of ticks fed on lumpy skin disease virus-infected cattle. *Experimental & Applied Acarology* 61 (1): 129–138. <https://doi.org/10.1007/s10493-013-9679-5>.
- Martin DP, Posada D, Crandall KA, Williamson C. 2005. A modified bootscan algorithm for automated identification of recombinant sequences and recombination breakpoints. *AIDS Res Hum Retroviruses*. 21(1): 98–102. <https://doi.org/10.1089/aid.2005.21.98>.
- Moje, N., A. Seifu, G. Hailegebreal, D. Shegu, S. Montagnaro, and G. Ferrara. 2024. Serological and community awareness study of lumpy skin disease in different agro-ecological zones of Sidama regional state. *Southern Ethiopia. Animals*. 14 (12): 1782. <https://doi.org/10.3390/ani14121782>.
- Moudgil, G., J. Chadha, L. Khullar, S. Chhibber, and K. Harjai. 2024. Lumpy skin disease: Insights into current status and geographical expansion of a transboundary viral disease. *Microbial Pathogenesis* 186 : 106485. <https://doi.org/10.1016/j.micpath.2023.106485>.
- Posada, D., and K. A. Crandall. 2001. Evaluation of methods for detecting recombination from DNA sequences: Computer simulations. *Proc Natl Acad Sci U S A* 98 (24): 13757–13762. <https://doi.org/10.1073/pnas.241370698>.
- Rhazi H, Safini N, Mikou K, Alhyane M, Lenk M, Tadaloui KO, Elharrak M. 2021. Comparative sensitivity study of primary cells, vero, OA3.Ts and ESH-L cell lines to lumpy skin disease, sheepox, and goatpox viruses detection and growth. *Journal of virological methods* 293: 114164. <https://doi.org/10.1016/j.jviromet.2021.114164>.
- Saegerman, C., S. Bertagnoli, G. Meyer, J. P. Ganière, P. Caufour, K. De Clercq, P. Jacquet, G. Fournié, C. Hautefeuille, F. Etoire, and J. Casal. 2018. Risk of introduction of lumpy skin disease in France by the import of vectors in animal trucks. *PLoS ONE* 13 (6): e0198506. <https://doi.org/10.1371/journal.pone.0198506>.
- Shumilova, I., A. Nesterov, O. Byadovskaya, P. Prutnikov, D. B. Wallace, M. Mokeeva, V. Pronin, A. Kononov, I. Chvala, and A. Sprygin. 2022. A recombinant vaccine-like strain of lumpy skin disease virus causes low-level infection of cattle through virus-inoculated feed. *Pathogens* 11 (8): 920. <https://doi.org/10.3390/pathogens11080920>.
- Smaraki, N., H. R. Jogi, D. J. Kamothi, and H. H. Savsani. 2024. An insight into emergence of lumpy skin disease virus: A threat to Indian cattle. *Archives of Microbiology* 206 (5): 210. <https://doi.org/10.1007/s00203-024-03932-6>.
- Song, Y., O. Zuo, G. Zhang, J. Hu, Z. Tian, G. Guan, J. Luo, H. Yin, Y. Shang, and J. Du. 2024. Emergence of lumpy skin disease virus infection in yaks, cattle-yaks, and cattle on the Qinghai-Xizang plateau of China. *Transboundary*

- and Emerging Diseases 2024:2383886. <https://doi.org/10.1155/2024/2383886>.
- Sprygin, A., E. Artyuchova, Y. Babin, P. Prutnikov, E. Kostrova, O. Byadovskaya, and A. Kononov. 2018a. Epidemiological characterization of lumpy skin disease outbreaks in Russia in 2016. *Transboundary and Emerging Diseases* 65 (6): 1514–1521. <https://doi.org/10.1111/tbed.12889>.
- Sprygin, A., Y. Babin, Y. Pestova, S. Kononova, D. B. Wallace, A. Van Schalkwyk, O. Byadovskaya, V. Diev, D. Lozovoy, and A. Kononov. 2018b. Analysis and insights into recombination signals in lumpy skin disease virus recovered in the field. *PLoS ONE* 13 (12): e0207480. <https://doi.org/10.1371/journal.pone.0207480>.
- Sprygin, A., Y. Pestova, O. Bjadovskaya, P. Prutnikov, N. Zinyakov, S. Kononova, O. Ruchnova, D. Lozovoy, I. Chvala, and A. Kononov. 2020. Evidence of recombination of vaccine strains of lumpy skin disease virus with field strains, causing disease. *PLoS ONE* 15 (5): e0232584. <https://doi.org/10.1371/journal.pone.0232584>.
- Sprygin A, Pestova Y, Prutnikov P, Kononov A. 2018. Detection of vaccine-like lumpy skin disease virus in cattle and *Musca domestica* L. flies in an outbreak of lumpy skin disease in Russia in 2017. *Transboundary and emerging diseases* 65(5): 1137–1144. <https://doi.org/10.1111/tbed.12897>.
- Sudhakar, S. B., N. Mishra, S. Kalaiyarasu, S. K. Jhade, and V. P. Singh. 2022. Genetic and phylogenetic analysis of lumpy skin disease viruses (LSDV) isolated from the first and subsequent field outbreaks in India during 2019 reveals close proximity with unique signatures of historical Kenyan NI-2490/Kenya/KSGP-like field strains. *Transboundary and Emerging Diseases* 69 (4): e451–e462. <https://doi.org/10.1111/tbed.14322>.
- Tran, H. T. T., A. D. Truong, A. K. Dang, D. V. Ly, C. T. Nguyen, N. T. Chu, T. V. Hoang, H. T. Nguyen, V. T. Nguyen, and H. V. Dang. 2021. Lumpy skin disease outbreaks in Vietnam, 2020. *Transboundary and Emerging Diseases* 68 (3): 977–980. <https://doi.org/10.1111/tbed.14022>.
- Vandenbussche, F., E. Mathijs, W. Philips, M. Saduakassova, I. De Leeuw, A. Sul-tanov, A. Haegeman, and K. De Clercq. 2022. Recombinant LSDV strains in Asia: Vaccine spillover or natural emergence? *Viruses* 14 (7): 1429. <https://doi.org/10.3390/v14071429>.
- Wang, J., Z. Xu, Z. Wang, Q. Li, X. Liang, S. Ye, K. Cheng, L. Xu, J. Mao, Z. Wang, W. Meng, Y. Sun, K. Jia, and S. Li. 2022. Isolation, identification and phylogenetic analysis of lumpy skin disease virus strain of outbreak in Guangdong, China. *Transboundary and Emerging Diseases* 69 (5): e2291–e2301. <https://doi.org/10.1111/tbed.14570>.
- Wei, Y. R., W. G. Ma, P. Wang, W. Wang, X. H. Su, X. Y. Yang, X. Y. Mi, J. Y. Wu, and J. Huang. 2023. Retrospective genomic analysis of the first lumpy skin disease virus outbreak in China (2019). *Frontiers in Veterinary Science* 9:1073648. <https://doi.org/10.3389/fvets.2022.1073648>.
- Whittle, L., R. Chapman, and A. L. Williamson. 2023. Lumpy skin disease—an emerging cattle disease in Europe and Asia. *Vaccines* 11 (3): 578. <https://doi.org/10.3390/vaccines11030578>.
- WOAH, Manual of diagnostic tests and vaccines for terrestrial animals 2023—lumpy skin diseases, WOAH Terrestrial Manual, Paris, 2023.
- Xu X, Zhao W, Xiang Z, Wang C, Qi M, Zhang S, Geng Y, Zhao Y, Yang K, Zhang Y, Guo A, Chen Y. 2024. Prevalence, molecular characteristics and virulence identification of bovine parainfluenza virus type 3 in China. *Viruses* 16(3): 402. <https://doi.org/10.3390/v16030402>.
- Yuan, X. W., H. Zhao, W. F. Ji, X. H. Yan, Z. J. Xiang, L. Yang, Y. C. Geng, Y. Y. Chen, J. G. Chen, X. Chen, L. Zhang, C. M. Hu, and A. Z. Guo. 2024. Preparation of a monoclonal antibody against recombinant LSDV034 protein and its application in detecting lumpy skin disease virus through a competitive enzyme-linked immunosorbent assay (cELISA). *Animal Diseases* 4 (1): 23. <https://doi.org/10.1186/s44149-024-00126-x>.
- Yuan XW, Wang Y, Adili Abulaiti, Li JK, Chen YY, Guo AZ. 2023. Research progress on prevalence, prevention and control of lumpy skin disease in cattle. *Journal of Huazhong Agricultural University* 42 (02): 9–16. <https://doi.org/10.13300/j.cnki.hnlkxb.2023.02.002>.
- Zaghoul M, Azooz M, Ali S, Soliman H, Sayed M, Kafafy M, Morsy A. 2022. Sequencing and phylogenetic analysis of GPCR, RPO30, P32 and EEV glycoprotein genes of lumpy skin disease virus recent isolates in Egypt. *Journal of Virological Sciences* 1: 1–11. <https://doi.org/10.17582/journal.jvs/sp1.1.11>.
- Zhang, M. M., Y. J. Sun, W. X. Liu, R. Q. Liu, X. J. Wang, and Z. G. Bu. 2020. Isolation and identification of lumpy skin disease virus from the first outbreak in China. *Chinese Journal of Preventive Veterinary Medicine* 42 (10): 1058–1061. <https://doi.org/10.3969/j.issn.1008-0589.202001025>.
- Zhou ZY, Du JG, Xin RL, Zhang JW, Pan CF, Yin CS, Chen XY, Zhu Z. 2024. Isolation and identification of three lumpy skin disease viruses in China and their GPCR gene analysis. *Acta Veterinaria et Zootechnica Sinica* 1–19. <https://doi.org/10.11843/j.issn.0366-6964.2024.12.025>.

Publisher's Note

Springer Nature remains neutral with regard to jurisdictional claims in published maps and institutional affiliations.